Appl Phys A (2013) 111:853–859
DOI 10.1007/s00339-012-7298-3

Applied Physics A
Materials Science & Processing

Co_xAg_{1-x} core–shell nanoparticles: magnetic and magneto-optical studies

B. Kalska-Szostko · M. Hilgendorff · M. Giersig · P. Fumagalli

Received: 5 June 2012 / Accepted: 23 September 2012 / Published online: 10 October 2012

Abstract The magneto-optical properties of 14-nm Co_x-Ag_{1-x} core–shell nanoparticles ($x = 0.7$, 0.8, and 0.35) deposited on different substrates are investigated at room temperature in the photon-energy range from 0.8 to 4.8 eV. Particles with low Ag content show spectra very similar to pure Co nanoparticles while particles with high Ag content have totally different features, where the Ag plasma edge dominates the spectra. The spectral features of the polar Kerr rotation depend on particle composition. The ageing process and development of an oxide layer influence the particles' core–shell structures and magnetization curves. Co-rich particles exhibit lower resistance to the oxidation process as compared to Ag-rich ones. The quality of the nanoparticles was checked by transmission electron microscopy in respect of time scale.

1 Introduction

For several decades, scientists have been working hard to prepare well-defined small magnetic particles. Nanoparticles exhibit interesting magnetic properties, which define them as good candidates for numerous applications in a variety of areas of human life such as recording media, biology, chemistry, cosmetics, or optics. The particles can be prepared in various ways ranging from vacuum techniques to chemical methods. In addition, nanostructures can be embedded in a matrix (metal or insulator) or used as a powder or in a colloidal form [1]. The main effort is dedicated to size-tunable particle preparation. A key issue for most applications is that the particles must be monodisperse and possess internal structure easily controllable by sample preparation [2]. Especially high-density magnetic recording media and magneto-optical storage media demand well-defined nanostructures.

For a long time, scientists were trying to prepare particles with well-defined size which are stable and less reactive to oxygen than pure elements. So, bimetallic, hybrid, or composite materials became a very interesting topic of such investigations [3] as they show dependence of the physical properties on composition. Studies of thin films and granular materials prove the influence of non-magnetic noble materials on 3d materials and vice versa. For example, magnetism can be induced in noble elements due to the presence of 3d elements in the system [4, 5]. In addition, some theoretical investigations predicted the existence of metastable phases in the case of low-dimensional systems such as Ag_3Co in thin films [6]. Therefore, it is interesting to prepare particles with large magnetic moment and large anisotropy which are stable in air. This presents an essential requirement for nanoparticles used in applications [7, 8]. Recently, bimetallic core–shell particles were synthesized using colloidal chemistry methods [9].

In this paper, we would like to present room-temperature magneto-optical Kerr effect (MOKE) studies of 14 ± 2 nm Co_xAg_{1-x} composite particles with composition x ranging from 0.35 to 0.8 as a complementary description of magnetic properties of the AgCo system.

B. Kalska-Szostko (✉)
Institute of Chemistry, University of Bialystok, Hurtowa 1, 15-399 Bialystok, Poland
e-mail: kalska@uwb.edu.pl

M. Hilgendorff · M. Giersig · P. Fumagalli
Institut für Experimentalphysik, Freie Universität Berlin, Arnimallee 14, 14195 Berlin, Germany

2 Experimental

Co_xAg_{1-x} composite particles were prepared by the standard Schlenck technique, for details see Ref. [9], based on thermal decomposition of dicobalt octacarbonyl in combination with a transmetalation reaction with water-free $AgClO_4$using oleic acid and tridodecylamine as a surfactant. The samples can be prepared with different Co-to-Ag molar ratios. The samples used for MOKE measurements had a Co content of about $x = 0.35$, 0.7, and 0.8, which is larger as compared to those mentioned in Ref. [9]. For structural characterization, transmission electron microscopy (TEM) images were taken.

The starting colloidal solution of an approximate concentration of 0.01 mol was diluted four times and thereafter dispersed in toluene. A drop of about 3–5 µl of the final solution was deposited on Cu, Au, or Al substrates and left for spontaneous evaporation. In order to induce structured arrangements of particles, an external magnetic field of 0.5 T was applied parallel or perpendicular to the sample plane.

The MOKE measurements were taken at room temperature at an angle of incidence of less than 5° with respect to the sample surface normal with a spectrometer working in an energy range of 0.8–4.8 eV. A sketch of the equipment is given in Fig. 1. An Al mirror was applied as a reference in order to compensate for the influence of Faraday rotation from the optical components of the setup. To cancel out the influence of stress-induced birefringence effects, all measurements except hysteresis curves were taken in both magnetic-field directions at ± 1.6 T and subtracted from each other. Two kind of light sources (halogen lamp for infrared and visual and xenon high-pressure lamp for ultraviolet ranges) are used and three different detectors for infrared, near-infrared/visual, and ultraviolet energy ranges, respectively. The sensitivity of the method is 0.002 deg [10].

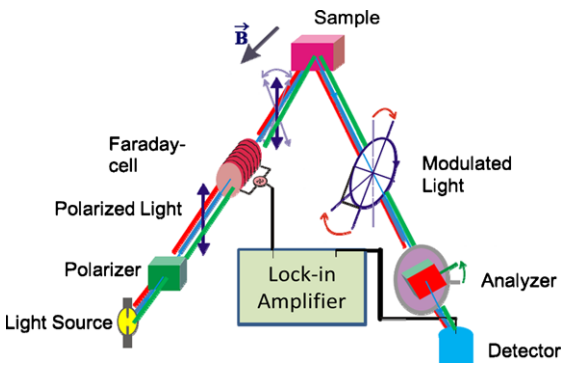

Fig. 1 Sketch of the polar Kerr spectrometer

3 Results and discussion

3.1 Transmission electron microscopy (TEM)

The particles studied are chemically very stable in air if the concentration of Co is less than $x = 0.5$. They do not show any traces of developing a CoO phase [9]. However, they are not so stable with respect to physical properties when containing more Co. In Fig. 2, two TEM images are shown taken from the same solution with a delay of nine months. Just after preparation, the solution is homogeneous and the particles have a rather spherical structure. After nine months, the homogeneity of the particles has decreased as compared to freshly prepared samples. The TEM images show an indication of phase separation inside the particles probably due to an oxidation process or polycrystallinity of the samples as reported in Ref. [11]. The average diameter of the particles discussed in this work was found to be 14 nm with a standard deviation of 16 % as calculated from a Gaussian distribution, $\overline{r} = (\sum_i^n r_i^3/n)^{1/3}$, where r_i is the radius of the ith particle and n is the number of particles taken into account, and has not changed with time as seen in Fig. 2b. In Fig. 2b, different contrast can be seen inside separate particles but CoO was not detected by high-resolution TEM (HRTEM). Particle distance in various samples should be the same since it is governed by substrate chemistry and the stabilization agents in all samples were the same.

Previous studies with HRTEM show polycrystalline face-centered-cubic (fcc) structure of Co and Ag with very well defined Co shell and Ag core [9]. Neither evidence of alloying nor existence of a CoO shell were found.

3.2 Magneto-optical Kerr effect (MOKE)

The reproducibility test depicted in Fig. 3a confirms very good sample homogeneity if deposited on the same type of substrate (as an example, an Al substrate was used). The values differ by about 20 % but the features are exactly the same.

In Fig. 3b, spectra of Co_xAg_{1-x} composite particles deposited on Al substrates from three different solutions containing a Co composition of $x = 0.35$, 0.7, and 0.8 are collected at room temperature. For the lowest Co composition $x = 0.35$ (■), the polar Kerr rotation is very small. Despite the particle size of 14 nm, the Co shell is only a thin layer of about 2 nm [9], which is not thick enough to develop ferromagnetism at room temperature. The only pronounced feature in the spectrum at 4.0 eV is produced by the Ag plasma edge. This feature is observed in any sample containing Ag. Note that the sharp feature in the polar Kerr rotation at 3 eV is an experimental artifact due to the change of optical filter and detector at that particular energy.

In order to corroborate the nature of the plasma peak at 4 eV, we plot in Fig. 3c the reflectivity spectra measured at

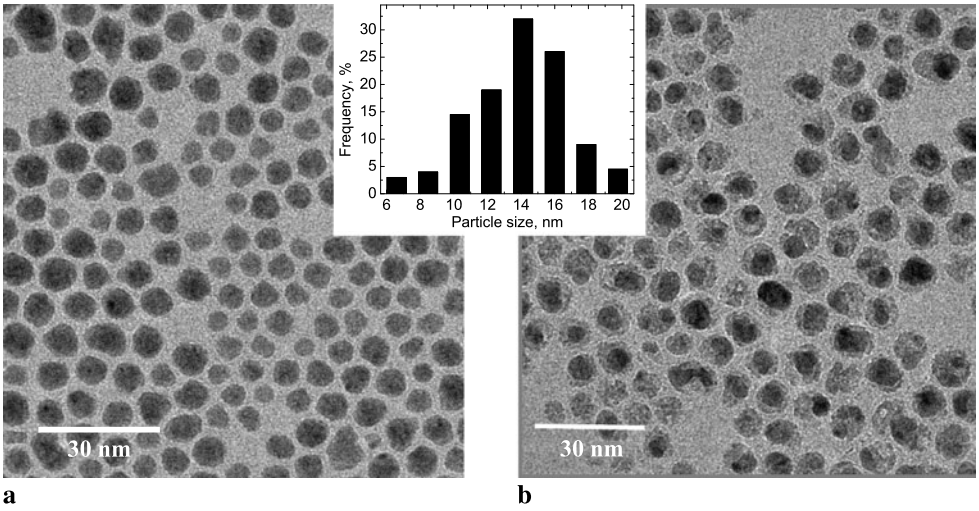

Fig. 2 TEM images of $Co_{0.7}Ag_{0.3}$ particles: (**a**) freshly prepared and (**b**) nine months after preparation. *Inset in (a–b)*: size distribution

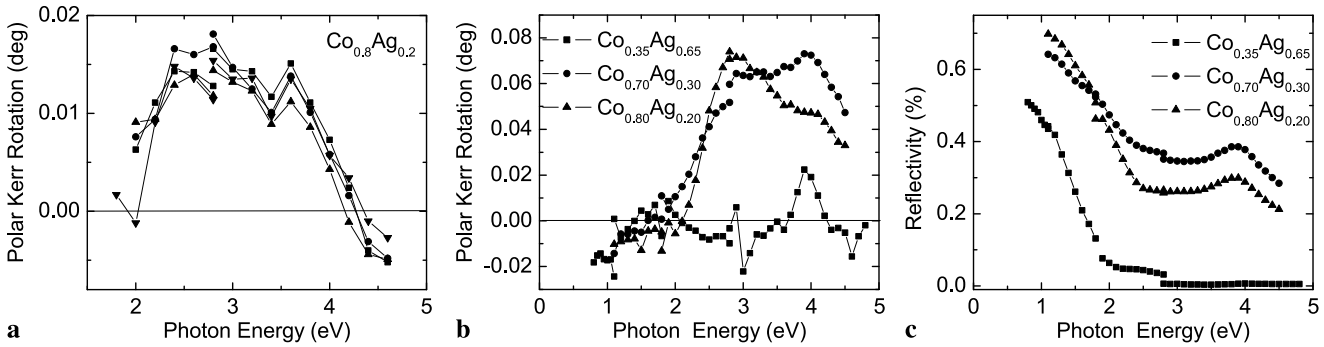

Fig. 3 (**a**) Reproducibility test of samples prepared of particles with Co content $x = 0.8$; (**b**) MOKE and (**c**) reflectivity spectra of samples prepared of particles with Co content $x = 0.35$, 0.7, and 0.8 (on Al substrate)

near-normal incidence. They show indeed pronounced features at the Ag plasma edge at 4 eV.

For particles with higher Co content, $x = 0.7$ (●) and 0.8 (▲), we notice in Fig. 3b an influence of particle composition on the polar Kerr rotation spectra expressed by an additional peak around 3 eV. The ratio of the magnitudes of the peaks at 3 and 4 eV is different. For a smaller amount of Ag, i.e. $x = 0.8$, we do not observe a pronounced plasma peak of Ag but a strong influence of Co at 3 eV. For the sample with $x = 0.7$, the dominant peak is around 4 eV. As mentioned before, the 4-eV peak is due to the optical properties of Ag and can also be seen in the reflectivity curves in Fig. 3c.

All Co_xAg_{1-x} MOKE spectra can be divided into two regions, one below and one above 2 eV. Below 2 eV, the MOKE signal has a negative sign as in thin films [12, 13] and bulk Co [14]. This was discussed thoroughly in Ref. [15]. Above 2 eV, the signal changes sign to positive. This behavior is unique to nanoparticle systems due to the competition between scattering and reflection phenomena [15].

The composite particles were deposited on different types of substrates to check if there is any influence on the polar Kerr rotation from the substrate, as was seen before for pure Co particles [15]. As is evident from Fig. 4, the dependence of the polar Kerr spectra on the substrate exists but is not as large as in the pure Co-nanoparticle case. In general, the polar Kerr rotation for single-phase particles is almost three times larger than for Co_xAg_{1-x} (for the same particle concentration). The polar Kerr rotation spectra show rather a dependence on Co composition than on substrate material, as can be seen for $x = 0.7$ and 0.8 in Fig. 4a, and c, respectively. The samples deposited on Cu have the same polar Kerr rotation regardless if the Cu buffer layer was deposited on glass or on Si. It is also noticed that for the samples with $x = 0.7$ the value of the polar Kerr rotation from particles deposited on Cu is about 40 % larger as compared to samples deposited on another material such as Al or Au. The same trend is seen for the samples with $x = 0.8$, except that the highest rotation is here achieved on Al substrates.

Discussing the origin of the structures in the Kerr spectra, the feature around 3 eV is most likely connected with the

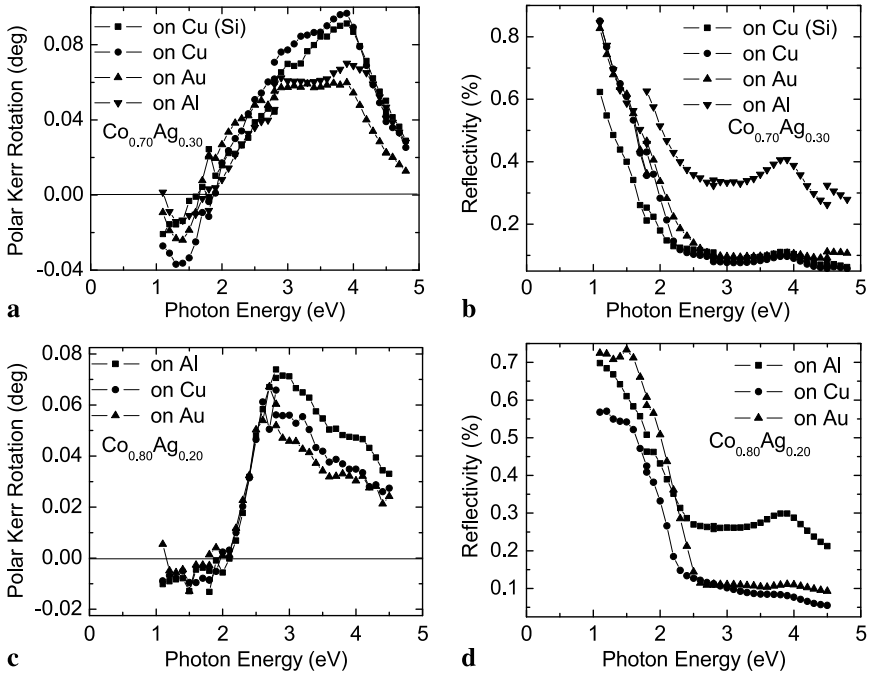

Fig. 4 (**a**), (**c**) MOKE and (**b**), (**d**) reflectivity spectra of samples prepared of particles with Co composition $x = 0.7$ and 0.8, respectively, deposited on different substrates

particle size, since the position of this peak is independent of the substrate used. The origin of the feature is an optical enhancement effect as is evident from Fig. 4b and d where the reflectivity drops strongly for both Co concentrations up to approximately 3 eV. It is well known that a pronounced decrease in reflectivity will lead to defined structures in the polar Kerr spectrum [15, 16]. The feature at 4 eV, on the other hand, is related to the Ag plasma edge, as discussed before. From this results a dependence of peak intensity on composition. A similar phenomenon was observed as increase of optical density with increase of Ag particle content in a mixture of Ag and Co particles (not shown). A shift and quenching of plasmons with change of Co content in composite particles has been observed before [15]. However, the measurements we performed here are not sensitive enough to see a difference in energy of the plasma edge with composition. At energies below 2 eV, the spectrum changes sign to negative and we can see a local minimum at about 1.4 eV reminiscent of the spectrum of pure Co particles [15].

Similarly, the position of the main Co peak going from Al to Cu and Au substrates shifts toward lower energy (it varies between 3.3 and 2.7 eV, respectively). Apparently, the modulation of Kerr rotation is sensitive to the underlying substrate material, as was shown for thin films [17]. Such behavior was also observed for pure Co particles [15]. The peak shift is more pronounced in samples with higher Co content where the Ag plasma-edge peak is weaker. Particles deposited on Cu have the same polar Kerr rotation and differ from Au and Al substrates. Less influence from the substrate composition can be due to fact that Co_xAg_{1-x} particles are larger as compared to pure Co particles and the observed features on the substrates are no longer critical for sample deposition and particle interaction. The signal is much weaker, so any change has also smaller values.

Co_xAg_{1-x} composite particles (see Fig. 5) also show a weak influence from the way of deposition (i.e. with or without the presence of a magnetic field). The case of a perpendicular magnetic field has the largest polar Kerr rotation for particles with $x = 0.7$. This kind of deposition should lead to better distribution of the particles. Hence, more homogeneous films of particles should be created. The relative relation between the peaks is similar to the one obtained with an external magnetic field. Therefore, the MOKE signal does not depend on the way of drying of the sample but only on the composition of the particles.

The particles do not show out-of-plane magnetization as is observed for pure Co particles [14], see Fig. 6. By fitting a Langevin function to the hysteresis loops obtained for different compositions of the Co_xAg_{1-x} particles, the effective magnetic part is much larger than for pure Co of the same size. This could indicate that the presence of Ag in the particles suppresses the oxidation process.

3.3 Magnetization measurements

3.3.1 $Co_{0.35}Ag_{0.65}$

The temperature dependence of the zero-field-cooled (ZFC)/field-cooled (FC) curve does not show any transition up to 180 K as plotted in Fig. 7a. A possible explanation of such behavior is that the main portion of the solution is superparamagnetic, dominating the magnetization at only 10 K. But

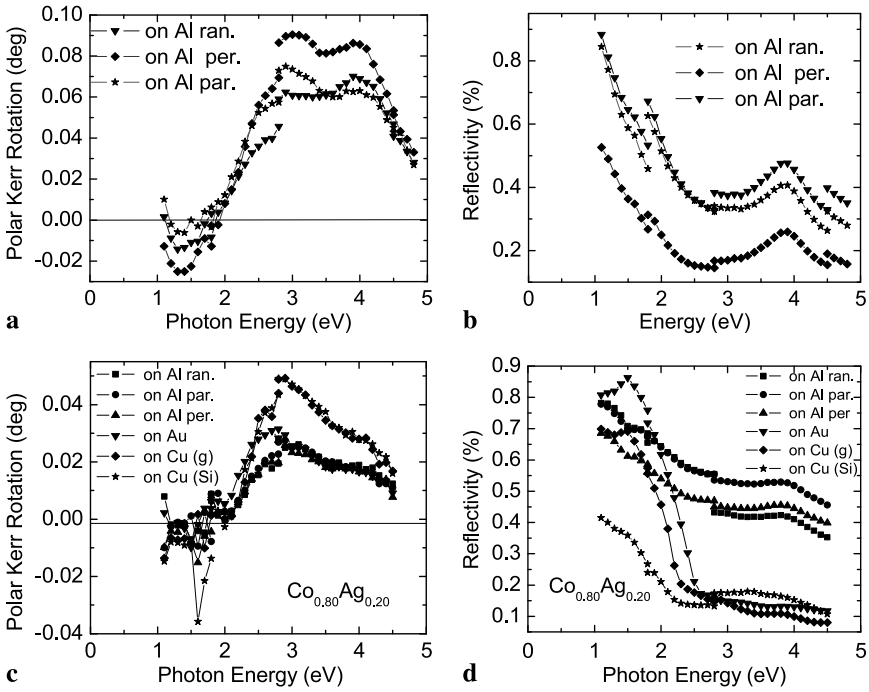

Fig. 5 (**a**), (**c**) MOKE and (**b**), (**d**) reflectivity spectra of samples prepared of particles with Co content $x = 0.7$ and 0.8, respectively, in the presence of a magnetic field

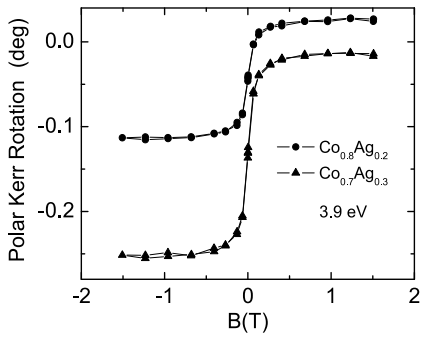

Fig. 6 MOKE hysteresis curve of a samples prepared of particles with Co content $x = 0.7$ and 0.8, respectively, taken at 3.9 eV (on Al substrate)

there are a few (probably larger particles or particles without a Ag core) that are ferromagnetic, dominating the magnetization at higher temperatures. In addition, we always have the strong diamagnetic contribution of the Ag cores.

The FC and ZFC magnetization loops measured at 10 K are very similar. However, comparing the magnetization loops measured at 10, 40, and 100 K, a different behavior is evident (Fig. 7b–d). At 10 K, the magnetization does not saturate up to 5.5 T, suggesting paramagnetic or rather superparamagnetic behavior of the particles. No clear indication of ferromagnetic interaction (hysteresis) was detected. There is a more pronounced ferromagnetic contribution visible at 40 and 100 K (steep, step-like increase of magnetization around zero field) besides an increasing diamagnetic contribution (negative slope) which originates from the core of the particle consisting of diamagnetic silver. At lower temperature, the observed negative slope is smaller, probably due to a paramagnetic contribution of the Co shell.

3.3.2 $Co_{0.8}Ag_{0.2}$

As shown in Fig. 8, the magnetization loop at 10 K exhibits a hysteresis for this sample, in contrast to Fig. 7. The curve shows an asymmetry in shape. When the field is rising, the magnetization of the particles is harder to align along the field direction and saturation is not reached at the maximum field of 5.5 T. When the field is decreasing, the magnetization of the particles is following the magnetic field more easily. The coercive field for $Co_{0.8}Ag_{0.2}$ at 10 K is 0.25 T and the remanence is 28 % of the saturation magnetization. Such behavior can indicate to some extent interparticle interaction. This is a quite possible scenario especially since ZFC-FC magnetization curves were taken for unsupported particles and magnetic interaction can bring particles closer together as compared to the distance in a quasi-two-dimensional array of a dried droplet.

The particles show for samples with a Co content $x > 0.7$ a large exchange-bias (EB) effect which is quite surprising for these samples. Previous studies show that particles with Co content $x = 0.3$ to 0.4 are oxide free for quite a long time [9]. Previous analysis of composition and structure of these core–shell particles has not indicated any oxidation. However, the analysis is not sensitive enough to reveal a very thin layer of oxide. The exchange-bias effect is due to an

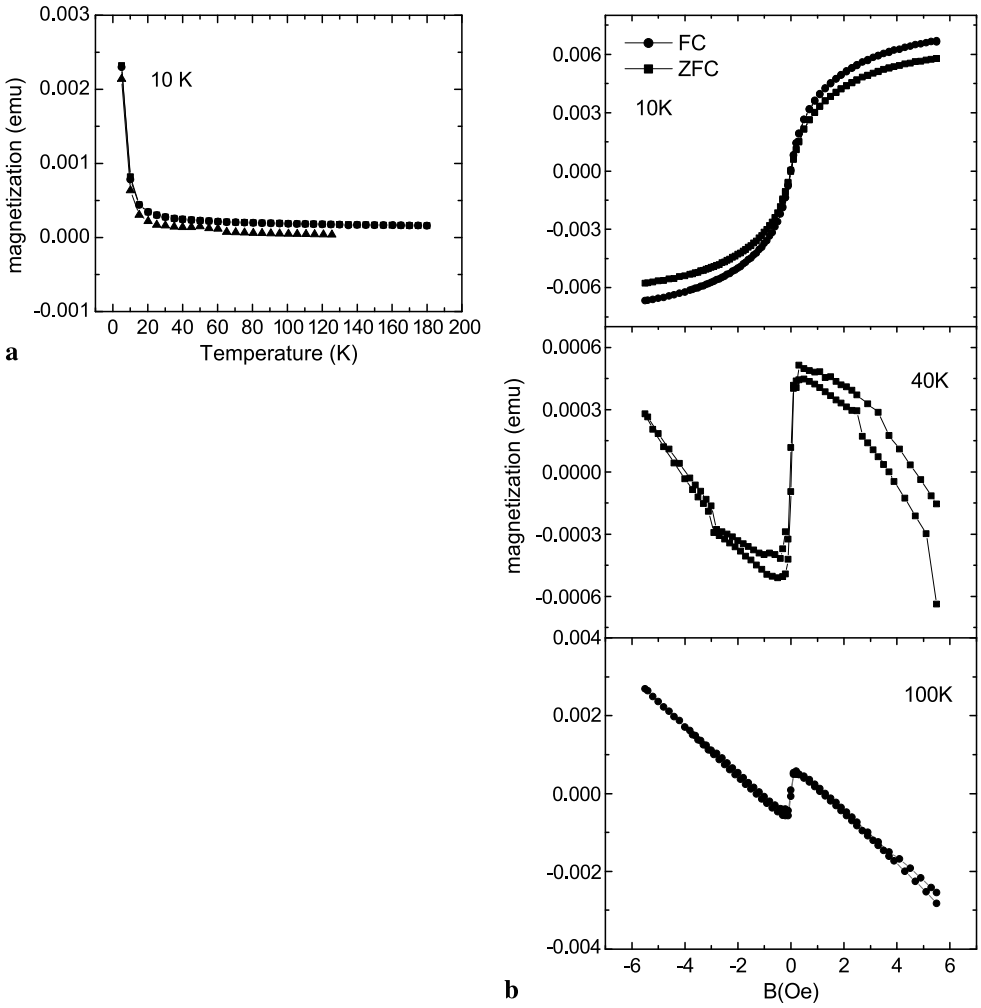

Fig. 7 (**a**) ZFC-FC SQUID magnetization dependence, (**b**) SQUID hysteresis loops taken at 10, 40, and 100 K, respectively, of particles with Co content $x = 0.35$

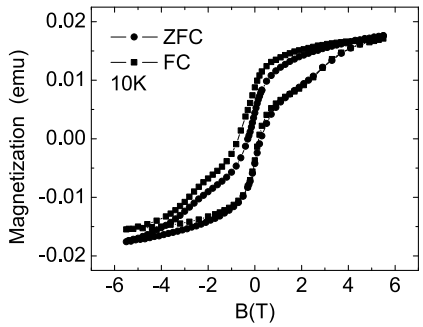

Fig. 8 ZFC-FC SQUID hysteresis loops taken at 10 K for particles with Co content $x = 0.8$

interaction between ferromagnetically ordered Co and antiferromagnetic CoO, corroborating a thin CoO layer on the surface of the core–shell particles [12, 15]. The strength of the exchange-bias effect is not as high as observed in pure Co particles, where a value of 0.8 T was estimated at 10 K [18], but it is too strong (around 0.25 T) to be mixed up with other phenomena. Table 1 summarizes what was observed before in the system including our findings.

4 Conclusion

We believe that the rotation changes sign as compared to a pure Co thin layer because we have a combination of scattering and reflection from the substrate and the particles leading to an optical enhancement effect.

The Co_xAg_{1-x} core–shell particles with Co content $x = 0.7$ and 0.8 are much less stable than such with smaller Co content ($x \leq 0.5$). The films reproduce the surface and distribution dependence on polar Kerr rotation as previously seen for pure Co particles. A pronounced Ag plasma-edge peak is seen in the MOKE spectra. An exchange-bias effect observed for Co content $x = 0.8$ can be explained by the development of a CoO shell at the particle surface which is not observable for Ag-rich samples.

Table 1 Summary of the experimental results of Co_xAg_{1-x} core–shell nanoparticles

Sample	Particle size	Type of experiment	Results	Reference
$Co_{70}Ag_{30}$	18 nm	SQUID	Spin disorder and enhancement of surface anisotropy	[19]
$Co_{45}Ag_{55}$	11.5 nm	Electron energy-loss spectroscopy	Confirmation of $Ag_{core}Co_{shell}$ structure	[9]
$Co_{45}Ag_{55}$, $Co_{70}Ag_{30}$	13.1 nm, 15.2 nm	SQUID	Lack of saturation magnetization up to 5.5 T	[11]
$Co_{35}Ag_{65}$, $Co_{70}Ag_{30}$, $Co_{80}Ag_{20}$	14 nm	MOKE, SQUID	Below Co content 0.7 no EB was observed. For 0.8 Co EB is present, suggesting presence of oxide layer. MOKE results very similar to pure Co nanoparticles	Our results

The TEM images give evidence for an ageing process going on in the particles via creation of oxides or phase separation in the particles. Both of them can change the contrast in the particles as seen in the TEM images. Therefore, for higher Co concentration the stability of the particles must be improved in the near future.

Acknowledgements We acknowledge the support of the European Union under contract no. HPRN-CT-1999-00150. B.K. would like to thank R. Feyerherm for SQUID measurements and N. Sobal for particle fabrication.

References

1. J.R. Childress, C.L. Chien, J. Appl. Phys. **70**, 5885 (1991)
2. C.B. Murray, S. Sun, H. Doyle, T. Betley, MES Bull. **December**, 985 (2001)
3. S.H. Liou, S. Malhotra, Z.S. Shan, D.J. Sellmyer, S. Nafis, J.A. Woollam, C.P. Reed, R.J. De Angelis, G.M. Chow, J. Appl. Phys. **70**, 5882 (1991)
4. M.E. McHenry, J.M. MacLern, D.P. Clougherty, J. Appl. Phys. **70**, 5932 (1991)
5. G.R. Harp, S.S.P. Parkin, W.L. O'Brien, B.P. Tonner, Phys. Rev. B **51**, 12037 (1995)
6. J.B. Liu, Z.F. Li, J.X. Zhang, B.X. Liu, G. Kresse, J. Hafner, Phys. Rev. B **64**, 054102 (2001)
7. R.D. Shull, L.H. Bennet, Nanostruct. Mater. **1**, 83 (1992)
8. G. Moraitis, H. Dreyssé, M.A. Khan, Phys. Rev. B **54**, 12037 (1996)
9. N.S. Sobal, M. Hilgendorff, H. Möhwald, M. Giersig, M. Spasova, T. Radetic, M. Farle, Nano Lett. **2**, 621 (2002)
10. P. Fumagalli, PhD thesis No. 9082, Swiss Federal Institute of Technology, 1990
11. O. Crisan, M. Angelakeris, K. Simeonidis, Th. Kehagias, Ph. Komninou, M. Giersig, N.K. Flevaris, Acta Mater. **54**, 5251 (2006)
12. B. Kalska, J.J. Paggel, P. Fumagalli, M. Hilgendorff, M. Giersig, J. Appl. Phys. **92**, 7481 (2002)
13. C. Müller, H. Lippitz, J.J. Paggel, P. Fumagalli, J. Appl. Phys. **91**, 7535 (2002)
14. J. Schoenes, in *Materials Science and Technology*, vol. 3, ed. by R.W. Cahn, P. Haasen, E.J. Kramer (Springer, Berlin, 1991)
15. B. Kalska, K. Schwinge, J.J. Paggel, P. Fumagalli, M. Hilgendorff, M. Giersig, J. Appl. Phys. **98**, 044318 (2005)
16. P. Fumagalli, H. Munekata, Phys. Rev. B **53**, 15045 (1996)
17. H.R. Zhai, Y.B. Xu, M. Lu, Y.Z. Miao, K.L. Hougue, H.M. Niak, M. Ahmad, G.L. Dunifer, J. Appl. Phys. **70**, 5858 (1991)
18. B. Kalska, P. Fumagalli, M. Hilgendorff, M. Giersig, Mater. Chem. Phys. **112**(3), 1129 (2008)
19. O. Crisan, M. Angelakeris, N.K. Flevaris, N. Sobal, M. Giersig, Sens. Actuators A **106**, 130 (2003)